Chapter 2

Theory of Thermal Noise

2.1 Introduction

What we call thermal noise in LIGO's mirrors falls naturally into two broad categories of sources.

- Intrinsic (dissipative) noise is driven by thermal forcing from internal fluctuations. A mirror's *dissipation* describes coupling of a mechanical (or chemical, or electrical, etc...) motion to a heat reservoir. Just as this loss converts mechanical energy to thermal energy, random thermal fluctuations are spontaneously converted back to mechanical fluctuations, as described by the fluctuation-dissipation theorem (FDT) of Callen and Welton [29, 28]. Some types of thermal noise can be easily identified with temperature: thermal energy fluctuates[76, 78], and material properties such as length and index of refraction fluctuate with it.

- Extrinsic (non-dissipative) noise arises when externally imposed temperature variations drive thermal fluctuations. For instance, the mirror may absorb heat from a laser beam with fluctuating intensity, causing length changes by thermal expansion.

How these sources affect gravitational wave detection depends on where they appear. LIGO test masses are thin dielectric mirrors grown on top of thick, transparent substrates. Besides gravitational waves, the center of mass of the substrates can be moved by radiation pressure [99, 111], seismic noise [51, 105], changes in local gravity [65], and the people who work at the observatories [116]. But light senses the position of the mirror coating, not the position of the center of mass of the substrate, so there are also noise sources which appear at the mirror surfaces. Some types of mirror thermal noise, such as bulk internal friction (see §2.3.2), depend mostly on the properties of the substrate, while many depend on the coating, which is, in general, quite different from the substrate.

- The substrate has dimensions comparable to or larger than the laser spot size. It is a high-Q mechanical resonator made from high-purity, highly transparent glass or crystal.

- The dielectric mirror coating is only a few microns thick. While mirror substrates are carefully chosen for their low thermal noise and good performance, mirror coating materials are chosen mostly for their indices of refraction, and do not necessarily have high mechanical Qs or low thermal expansion.

The LIGO mirrors are made of quarter-wave stacks of Ta_2O_5/ SiO_2, and a major uncertainty in predicting thermal noise is in understanding the coatings themselves. Thermoelastic and photothermal noise are expected to depend on the coating's thermal expansion coefficient, thermal conductivity, and Young's modulus, and recent research into optical materials suggests that the thin films layers in the coatings may have physical properties quite different from those of bulk materials. For instance, the thermal expansion coefficient of stressed, sub-micron vapor deposited SiO_2 films has been observed in the range of 0.6 to 4×10^{-6}/K [5, 20, 30, 127], with elastic moduli from 40 - 60 GPa [68, 30], whereas bulk SiO_2 has a thermal expansion coefficient of 0.5×10^{-6}/K and an elastic modulus of 73 GPa [35]. The picture is murkier for Ta_2O_5, for which thin film thermal expansion coefficients of 3.6×10^{-6} [118] and -4.4×10^{-5} [66] have been observed. Recently, a bending-beam experiment measured the thermal expansion coefficient for Ta_2O_5 to be $5(\pm 2) \times 10^{-6}$ [25] in a LIGO silica/tantala multilayer coating.

The high thermal expansion of these materials could make them detrimental to test mass thermal noise, but switching to other materials is not likely to improve the situation. For Advanced LIGO [57], other coating materials have been considered [26, 108], such as Al_2O_3 (sapphire) and TiO_2. Sapphire, which has a crystalline bulk form, is believed to be amorphous as a thin film [80, 81], with a thermal conductivity that decreases with the film thickness [69]. While bulk sapphire has a thermal conductivity of 40 W/m-K [39], it has been observed to be only 3.3 W/m-K in a 2×10^{-7}m Al_2O_3 film [69]. The thermal expansion coefficient of TiO_2 thin films has been measured to be 50×10^{-6}/K [56], several times higher than in bulk samples [42].

This chapter enumerates the thermal noise effects that are expected to affect LIGO mirrors. Representative values of material properties are listed in Table 2.3. Calculations use SI units, unless explicitly noted. Symbols used in this section are listed below.

- r_0 laser spot radius ($1/e$ of central power), meters

- λ laser wavelength, 1.064×10^{-6} meters
- $f = \omega/2\pi$ measurement frequency, Hz
- $\rho\, C_v$ = density $\times$ heat capacity at constant volume, J/m^3
- κ thermal conductivity, W/mK
- σ Poisson's ratio, dimensionless
- α thermal expansion coefficient, $1/K$
- n index of refraction, dimensionless
- d coating thickness, usually $\sim 5 \times 10^{-6}$m
- $\beta = dn/dT$ temperature dependence of n, $1/K$
- ϕ loss angle, dimensionless
- r_t thermal diffusion length, $(\kappa/2\pi\rho C_v f)^{1/2}$
- E Elastic modulus (stress / strain), N/m^2
- P_{abs} power absorbed by a mirror, W
- k_B Boltzmann's constant, $1.39 \times 10^{-23} J/K$
- T temperature, generally $300K$

2.2 Background

2.2.1 Spectral densities

Random noise processes are described in terms of spectral densities [19]. The "one-sided" spectral density (defined for positive frequencies) of a random function $y(t)$ with mean value $\bar{y}$ is the limit of the square of the Fourier transform, defined by the equation

$$S_y(f) = \lim_{T\to\infty} \frac{2}{T} \left| \int_{-T/2}^{T/2} [y(t) - \bar{y}] e^{i2\pi f t}\, dt \right|^2 \tag{2.1}$$

The variance of y is the integral of $S_y(f)$ over positive frequencies.

$$\langle (y - \bar{y})^2 \rangle = \int_0^\infty S_y(f)\, df \tag{2.2}$$

The spectrum of the root-mean-square of the noise in y is $\sqrt{S_y(f)}$. A spectral density S_y has units of y^2 per Hz. To calculate $\langle (y - \bar{y})^2 \rangle$ in an observation, multiply S_y by the bandwidth of the measurement. To convert from a test mirror displacement spectral density to a LIGO interferometer strain, multiply by the factor $1/L^2$, where L is the length of the arm cavity.

2.2.2 Thermal length scales

All the thermal effects we will be considering depend on heat flow, so it's useful to define the thermal diffusion length $r_t = \sqrt{\kappa/\rho C_p 2\pi f}$ and its corresponding characteristic frequency $f_c = \frac{\kappa}{2\pi x^2 \rho C_p}$, where x is the characteristic length scale being measured, usually the spot radius r_0.

In a coating of thickness d made of two materials, where each layer is much thicker than the phonon mean free path, the effective thermal conductivity κ_e in the direction normal to the surface is dominated by the less conductive material [31].

$$\frac{d}{\kappa_e} \approx \frac{d_1}{\kappa_1} + \frac{d_2}{\kappa_2} \tag{2.3}$$

where κ_1 and κ_2 are the bulk conductivities. For a slab[1] of SiO_2/TiO_2, this would predict $\kappa_e \sim 2$ W/m-K. This puts the coating thermal diffusion length at around 100 microns at 100 Hz.

2.3 Intrinsic noise

Intrinsic thermal noise sources can be derived from the fluctuation-dissipation theorem when the dissipation mechanism is known. In cases where the dissipation mechanism is not obvious, noise effects can be identified by looking for material properties which depend on temperature, like thermal expansion and dn/dT. An introduction to the fluctuation-dissipation theorem is presented below, followed by a catalog of noise mechanisms.

[1] Al_2O_3 can be used instead of SiO_2, but sub-micron Al_2O_3 films have low thermal conductivity like SiO_2 [69].

2.3.1 The fluctuation-dissipation theorem

The fluctuation-dissipation theorem (Eq. 2.4) shows that thermodynamic noise is a consequence of any irreversible dissipation process [28, 29]. Given a generalized resistance, R to a driving force F, there will arise at non-zero temperatures a spontaneous fluctuation in F. Force and resistance are defined such that the resistance R is the real part of the impedance Z for some oscillatory force $F(f)$ that drives a coordinate q.

$$\langle F^2 \rangle = 4k_B T \int R(f)\, df = \int S_F(f)\, df \tag{2.4}$$

(2.5)

The relationship between F and R is defined by an impedance Z, defined by

$$F(f) = Z(f)\, \dot{q}(f) \tag{2.6}$$

$$F(f) = Z(f)\, i2\pi f q(f) \tag{2.7}$$

$$R(f) = \Re[Z(f)] \tag{2.8}$$

Knowing $S_F(f)$, we can find the spectral density of fluctuations in q.

$$\begin{aligned} S_q(f) &= \frac{S_F(f)}{Z^2 4\pi^2 f^2} \\ &= \frac{k_B T}{\pi^2 f^2} \frac{R}{|Z|^2} \\ &= \frac{k_B T}{\pi^2 f^2} \Re[\frac{1}{Z}] \end{aligned} \tag{2.9}$$

To obtain $\Re(1/Z)$, we can compute the average power converted to heat (the dissipation, P_d) due to a sinusuidal forcing function $F = F_0 \sin 2\pi f t$. This formula (Eq. 2.10) is provided by Levin [82] for the case where F and q are both distributed over the same Gaussian spot on the surface of the mirror, which leads directly to a solution

$$\Re[\frac{1}{Z(f)}] \quad = \quad \frac{2 \times Dissipated\,power}{F_0^2} \tag{2.10}$$

The dissipated power differs for each noise source, and is often frequency dependent. The key to understanding each source of thermal noise is identifying how an imaginary applied force (mechanical, electrical, magnetic, etc.) is converted into heat.

2.3.2 Bulk internal friction

Internal friction in solids was identified by Kimball and Li [73, 74], who described it as a phase shift between stress and strain. For historical reasons, this is what people commonly mean when they refer to "thermal" and "Brownian motion" noise. The Brownian motion interpretation comes from thinking of the mirror's recoil from its internal phonons, while the internal friction interpretation is a direct application of the fluctuation-dissipation theorem.

The figure of merit for internal friction in a material is its loss angle, ϕ, defined as the (small) phase of the complex elastic modulus $E = E_0(1+i\phi)$, where the loss angle and quality factor Q are related by $Q = 1/\phi$. One model for internal friction, first identified by identified by Saulson [110] as a source of noise for LIGO, is "structural damping," in which ϕ is independent of frequency. The assumption that $\phi(f)$ is constant may not be true (see [24, 13]) and there is evidence [124] to suggest that the loss angle of bulk materials increases with frequency.

There are two ways to calculate the noise from internal friction. In the Brownian motion model, each normal mode [111] has energy $k_B T$, and causes surface motion proportional to $f^{-1/2}$ below its resonant frequency. One can calculate the low-frequency thermal noise by numerically summing over the normal modes of the mirror [54].

The structural damping interpretation is easier to use. This was introduced by Levin [82] and identifies a force $F = F_0 \sin 2\pi f t$ as a periodic pressure on the mirror surface with a Gaussian spatial distribution matching that of the laser beam reflecting from the mirror. A method for extending Levin's half-space model to finite-sized mirrors was introduced by Bondu, Hello, and Vinet [45], and revised and extended by Liu and Thorne [88]. Using a Green's function technique, Nakagawa *et al.* [91, 92] derive the total interferometer thermal noise, accounting for multiple reflections in a Fabry-Perot interferometer or in a delay line interferometer. For a single mirror whose dimensions are much larger than the spot size, Levin derives the dissipated power.

$$\frac{Dissipated\ power}{F_0^2} \quad \propto \quad \frac{f\phi(f)(1-\sigma^2)}{E_0 r_0} \tag{2.11}$$

where E_0 is the real part of the elastic modulus. The spectral density of fluctuations given by Bondu, Hello, and Vinet is

$$S_{SD}^{bulk}(f) \quad = \quad \frac{4k_BT}{(2\pi)^{3/2}f}\frac{\phi(f)(1-\sigma^2)}{E_0 r_0} \tag{2.12}$$

Given this, the only difficulty in predicting structural damping noise is to identify the loss angle. Measurements in LIGO-like samples show that the Q of a low-loss fused silica mirror can vary by several orders of magnitude among resonant modes [27]. As Levin pointed out [82], this suggests that surface friction makes large contributions to mirror losses, but, depending on where they appear on the mirror, surface losses might not affect the bulk thermal noise. For instance, suspension point friction on the side of a mirror barrel might not figure highly in the vibrational modes that move the center of the mirror face.

It is generally believed that the loss angle that matters is that of the bulk material, and Numata's [94] data on BK7 (Q $\sim$ 4000) mirrors support this. In high-Q mirrors, the TNI (Ch. 4) shows that this could still be true, even with friction from wire supports and magnets. There are other noise sources associated with the test mass suspension [63], including viscous gas damping, and pendulum thermal noise.

2.3.3 Coating structural damping

The potential for structural damping in the coating to produce noise was introduced by Levin [82] and a theory developed by Nakagawa *et. al.* [93] and Harry *et. al.* [60]. Allowing for anisotropy in the coating, they characterize the coating structural damping by the loss angles of the mirror layers parallel and perpendicular to the mirror surface, $\phi_\parallel$ and $\phi_\perp$. Measurements made by Harry *et al.* [60] and Penn *et al.* [101] found $\phi_\parallel$ to be around 1×10^{-4} for Ta_2O_5/SiO_2 mirror coatings on superpolished fused silica and sapphire substrates, and measurements by Crooks *et. al.* found coating loss angles of $\sim 6 \times 10^{-5}$ for Ta_2O_5/Al_2O_3 mirror coatings on fused silica. They estimate the thermal noise contribution as

$$S_{SD}^{layer}(f) = \frac{2}{\pi^2}\frac{k_B T d}{E_{bulk} r_0^2 f}\left(\frac{E_{coating}}{E_{bulk}}\phi_{\parallel} + \frac{E_{bulk}}{E_{coating}}\phi_{\perp}\right) \tag{2.13}$$

This model is designed to explain noise on fused silica substrates and assumes the losses come from the bulk materials themselves, not from friction at boundaries. Values for $\phi_{\perp}$ are unknown and are assumed to be equal to $\phi_{\parallel}$.

2.3.4 Bulk thermoelastic noise

A system in equilibrium with a heat reservoir may have fluctuations in its energy E, according to the equation [104]

$$\begin{aligned} \langle(\Delta E)^2\rangle &= \frac{\partial^2 ln Z}{\partial \beta_t^2} \\ Z &= \sum_n e^{\beta_t E_n} \end{aligned} \tag{2.14}$$

where $\beta_t = 1/k_B T$ and Z is the partition function, summed over all possible states of the system. Since the mean energy can be written as $\bar{E} = -\frac{\partial}{\partial \beta_t} Z$, Eq. 2.14 can be written as

$$\langle(\Delta E)^2\rangle = k_B T^2 \left(\frac{\partial E}{\partial T}\right)_V \tag{2.15}$$

Temperature fluctuations are a convenient way to think about these energy fluctuations, by taking $\Delta E = C_v V \Delta T$. According to Kittel [76], this is not strictly correct, since temperature, by definition, does not fluctuate. Nevertheless, it is a powerful tool for understanding fluctuations in temperature-dependent parameters. For this purpose, one can use an effective temperature fluctuation for a region of volume V [78]

$$\langle(\Delta T)^2\rangle = \frac{k_B T^2}{\rho C_v V} \tag{2.16}$$

For instance, if the mirror substrate has a non-zero thermal expansion coefficient, these fluctuations will move its surface. Another way of thinking about this system is thermoelastic damping. Braginsky, Gorodetsky, and Vyatchanin (BGV99) [22] showed that a periodic pressure at the sur-

face of a material with non-zero thermal expansion leads to heat flux and energy dissipation. The fluctuation-dissipation theorem then relates the lost energy to the surface displacement. For laser spots significantly smaller than the mirror dimensions, the expected length noise is [32]

$$S_{\alpha,T}^{bulk}(f) = \frac{8}{\sqrt{2\pi}} \frac{\alpha^2(1+\sigma)^2 k_B T^2 r_0}{\kappa} \times \int_0^\infty du \int_{-\infty}^\infty dv \frac{\sqrt{2}u^3 e^{-u^2/2}}{\sqrt{\pi}(u^2+v^2)((u^2+v^2)^2+(f/f_c)^2)} \tag{2.17}$$

where $f_c = \frac{\kappa}{2\pi r_0^2 \rho C_p}$. In the limit of high frequencies or large spot sizes ($f \gg f_c$), Eq. 2.17 approaches the BGV99 prediction.

$$S_{\alpha,T}^{bulk}(f) = \frac{8}{\sqrt{2\pi}} \frac{\alpha^2(1+\sigma)^2 \kappa k_B T^2}{(2\pi\rho C_V)^2 r_0^3 f^2} \tag{2.18}$$

Where the spot size is comparable to the mirror dimensions (but still larger than the thermal diffusion length) and $f \gg f_c$, analytic approximations by Liu and Thorne [88] predict differences from the BGV99 formula on the order of 10-20%. This noise has been measured by Kenji Numata [94] in CaF_2 mirrors and agrees well with theory.

2.3.5 Coating thermoelastic noise

Thermodynamic fluctuations are local and depend on the volume of the affected region. Measured as an average over the entire test mass, the temperature is better defined than it is for a small region, say the volume of the dielectric mirror coating itself. These short-range temperature fluctuations are expected to be significant sources of noise for LIGO.

High-quality dielectric mirrors are made from alternating quarter-wave layers of high- and low-index materials. Preferred high-index compounds are Ta_2O_5 and TiO_2 which, as thin films, may have high thermal expansion and dn/dT coefficients [66, 56]. Preferred low-index compounds are SiO_2 and Al_2O_3.

To consider noise from the mirror coating, only the temperature changes near the surface of the mirror matter. The thermal diffusion length sets the length scale of regions with independently fluctuating temperatures, and a large laser spot will average the fluctuations of many of these regions.

If the coating has good thermal coupling to the substrate, the substrate and the coating can be expected to have the same temperature fluctuations. In this case, the coating may be thought of as a continuation of the substrate, just with a different thermal expansion. Braginsky and Vyatchanin

(BV03) [26] have estimated the spectral density of the surface fluctuations as observed by a Gaussian beam. For a uniform coating with thickness l, the temperature fluctuations are

$$S_{\Delta T}^{layer}(f) = \frac{\sqrt{2}k_B T^2}{\pi r_0^2 \sqrt{\kappa \rho C_v 2\pi f}} \tag{2.19}$$

and the thermal expansion averaged over a Gaussian beam is [26]

$$S_{\alpha,T}^{layer}(f) \quad = \quad \frac{4\sqrt{2}}{\pi} \frac{\alpha_{eff}^2 (1+\sigma)^2 d^2 k_B T^2}{r_0^2 \sqrt{\kappa \rho C_V 2\pi f}} \tag{2.20}$$

where d is the total layer thickness and α_{eff} is the coefficient of thermal expansion for the coating in the direction normal to the surface. A real dielectric mirror has upwards of 40 layers, and there could be a "bimetallic" stress effect to cause more surface displacement. By balancing the horizontal stresses, BV03 propose that the multilayer coating be treated by an effective thermal expansion coefficient.

$$\alpha_{eff} \quad = \quad \frac{\alpha_1 d_1}{d_1 + d_2} \frac{E_1(1-2\sigma)}{E(1-2\sigma_1)} + \frac{\alpha_2 d_2}{d_1 + d_2} \frac{E_2(1-2\sigma)}{E(1-2\sigma_2)} - \alpha_{bulk} \tag{2.21}$$

where d_1 and d_2 are individual layer thicknesses and the E's and σ's are the various elastic moduli and Poisson's ratios of the coating materials. Ignoring the Young's modulus and Poisson's ratio and assuming the lower values from Table 2.1, α_{eff} for a Ta_2O_5 / SiO_2 coating is 1.8×10^{-6}/K.

If the coating is much less stiff than the substrate, one might expect the coating to react as if it were compressed or stretched in the transverse plane. Then, simply by applying the definition of Poisson's ratio, the effective thermal expansion coefficient could take the form (see Eq. 7.12 in [78])

$$\alpha_{eff} \quad = \quad \frac{\alpha_1 d_1 (1+2\sigma_1)}{d_1 + d_2} + \frac{\alpha_2 d_2 (1+2\sigma_2)}{d_1 + d_2} - \alpha_{bulk} \tag{2.22}$$

Rowan and Fejer [108] present a different theory to account for differences in thermal diffusivity between the coating and substrate. Their estimate of the coating thermal expansion is

$$
\begin{aligned}
S_{\alpha,T}^{layer*} &= \frac{4k_BT^2}{\pi^2 f r_0^2}\frac{\rho_{layer}C_{layer}}{\rho_{bulk}^2 C_{bulk}^2}\alpha_{eff}^2 d(1+\sigma)^2 g(\omega) \qquad (2.23)\\
\alpha_{eff} &= \frac{\alpha_{layer}\rho_{layer}C_{bulk}}{2\rho_{bulk}C_{layer}(1-\sigma_{bulk})}\left(\frac{1+\sigma_{layer}}{1+\sigma_{bulk}} + (1-2\sigma_{bulk})\frac{E_{layer}}{E_{bulk}}\right) - \alpha_{bulk}\\
g(\omega) &= \Im\left[\frac{-\sinh(\sqrt{i\omega\tau})}{\sqrt{i\omega\tau}\left(\cosh(\sqrt{i\omega\tau}) + \sqrt{\frac{\kappa_{layer}\rho_{layer}C_{layer}}{\kappa_{bulk}\rho_{bulk}C_{bulk}}}\sinh(\sqrt{i\omega\tau})\right)}\right]
\end{aligned}
$$

where $\tau = d^2\rho C/\kappa$ for the coating. At high frequencies, $g(\omega)$ has a $f^{-1/2}$ dependence, and at $\omega = 1/\tau$, $g(\omega)$ is 0.26. Assuming that the material properties for the coating layers and the bulkare the same and taking the high-frequency limit, Eq. 2.23 differs from Eq. eq2:layertd by a factor of $1/\omega\tau$ (neglecting factors of order unity).

2.3.6 Coating thermorefractive noise

Fluctuations in the refractive index of the mirror coating layers also cause changes in the phase of the light they reflect. The formula for dn/dT noise follows directly from Eq. 2.20. For a dielectric mirror made from two materials with indices of refraction n_1 and n_2 and $\beta_i = dn_i/dT$ the length-equivalent noise was derived by BGV00 [23].

$$
\begin{aligned}
S_{\beta,T}^{layer}(f) &= \beta_{eff}^2\lambda^2\frac{\sqrt{2}k_BT^2}{\pi\, r_0^2\sqrt{2\pi\rho C_v\kappa f}} \qquad (2.24)\\
\beta_{eff} &= \frac{n_2 n_1(\beta_1+\beta_2)}{4(n_1^2-n_2^2)}
\end{aligned}
$$

The loss mechanism behind dn/dT noise may be electrocaloric dissipation [123], so it is possible thatS_β^{layer} and S_α^{layer} are at least partially uncorrelated, as both the lattice expansion and the temperature dependence of optical resonances affect dn/dT in glasses [49].

2.3.7 Bulk thermorefractive noise

Most GW Michelson interferometer designs involve passing light through at least one thick optic, the beamsplitter. As the index of refraction of the beamsplitter substrate depends on temperature, temperature fluctuations will impart phase fluctuations in the interferometer.

$$S^{\beta}_{\Delta\phi}(f) = \left(\frac{\beta l}{\lambda}\right)^2 \frac{\sqrt{2}k_B T^2}{\pi r_0^2 \sqrt{\rho C_v 2\pi f}} \tag{2.25}$$

where l is the mirror thickness. This could be a limiting noise source in an interferometer with high optical gain in the Michelson cavity (such as in GEO600[58]), but it is believed to not be a major problem for LIGO [123].

2.4 Photon-driven noise

Driven temperature fluctuations arise from the test mass being heated, such as by absorption of photons from a laser beam with intensity fluctuations. Photon-drive noise depends, of course, on the absorptivity of the mirror, which can depend strongly on the coating manufacturing process.

2.4.1 Bulk expansion

When a material absorbs light, it converts it to heat and thermal expansion ensues. This is commonly known as the "photothermal" effect, although a more specific name would be "photoelastic," to distinguish it from the photorefractive (dn/dT) effect.

The photothermal effect is used (particularly in the semiconductor industry) to measure thermal properties of materials [67, 95, 9]. A common configuration is the modulated photothermal deflection experiment [83, 10], in which a "pump" laser beam, chopped into a square wave, strikes a sample at normal incidence, while a "probe" beam strikes the sample at a glancing angle. The pump beam is partially absorbed by the sample, raising a blister, which is observed by deflection of the probe beam.

There is less work on transparent materials like the glasses and crystals used for making mirror substrates. An interferometer is a natural tool to study these, where the photothermal distance changes may be less than a nanometer. De Rosa et al. [106] have reported observation of the photothermal effect in low-absorption (0.5 ppm) dielectric mirrors made by Research Electro-Optics (REO[2]) [107]. Their study was done at low frequencies (10 mHz - 200 Hz), using two Fabry-Perot interferometers with fused silica mirrors, and appears to agree well with theory. Measurements of this effect in several types of mirror in a higher frequency band are presented in the following chapter.

[2]REO claims absorption of 10 ppm or less, which is sometimes used as a conservative estimate for LIGO. LIGO's specified limit on increase in optical absorption is 2 ppm/year [84]

For intensity fluctuations in the light absorbed by the mirror given by S_{abs}, the photothermal length change measured by an interferometer is [32]

$$S_{\alpha,P}(f) = \frac{2\alpha^2(1+\sigma)^2 S_{abs}}{\pi^2\kappa^2} \times \left[\frac{1}{\pi}\int_0^\infty du \int_{-\infty}^\infty dv [\frac{u^2 e^{-u^2/2}}{(u^2+v^2)(u^2+v^2+if/f_c)}]\right]^2 \quad (2.26)$$

At high frequencies or large laser spots ($f \gg f_c$), this function simplifies to [22]

$$S_{\alpha,P}^{bulk}(f) = \frac{\alpha^2(1+\sigma)^2}{2\pi^2}\frac{S_{abs}(f)}{(\rho C_V \pi r_0^2)^2 f^2} \quad (2.27)$$

The shot noise limit S_{abs} depends on the average power absorbed by the mirror $\bar{P}_{abs}$ and the photon energy $h\nu = hc/\lambda$. The average rate of photon absorption is $N = \bar{P}_{abs}/h\nu$, and, from Poisson statistics, the fluctuation in N is $\sqrt{N}$. Thus, the fluctuation in the absorbed power is $\sqrt{N}h\nu = \sqrt{\bar{P}_{abs}h\nu}$. The square of this gives the spectral density of the fluctuations, or simply $S_{abs} = \bar{P}_{abs}h\nu$.

2.4.2 Coating expansion

We would like to estimate how photon heating on a Gaussian spot at the mirror surface affects the temperature distribution $u(\vec{r}, t)$ throughout the mirror. At high frequencies, where r_t is less than the coating thickness, the coating expansion should behave like bulk thermal expansion, much like the situation described in §2.4.1. In the other limit, at low frequencies, the coating and the substrate should be at the same temperature, so that the coating's average length change just scales with substrate temperature, $\Delta x = \alpha_{layer} d\,\Delta T$. In between is a regime where the average coating and substrate temperatures may be different, and new models are needed. A calculation of the coating's thermal response in this range depends on how the thermal diffusivity $a^2 = \kappa/\rho C$ of the coating compares to that of the substrate.

Consider a two-dimensional model of a 5 micron SiO_2/TiO_2 coating on top of a sapphire or fused silica substrate, with heat applied steadily at a spot on the coating's surface and allowed to diffuse into the bulk. The heat flow patterns simulated with Matlab [114], shown in Fig. 2.1, are quite different for these two scenarios. In the sapphire case, heat diffuses slowly through the coating, and quickly through the substrate. In the coating, the heat flow does not have time to diffuse to the

Figure 2.1: Heat flow simulation created with Matlab and PDETool. A constant unit heat flow is applied to a 200 micron wide spot on at a mirror surface. Lines show contours of constant temperature. The scale shows the temperature in arbitrary units. The coating is 5 microns thick, an average of SiO_2 and TiO_2, with $\rho = 3200$ kg/m^3 - K, $C_v = 700$ J/kg-K, $\kappa = 2$ W/m-K (from Eq. 2.3). The mirror coating away from the heated spot does not conduct heat, and the bottom and sides, far away, have fixed T=0. A: Sapphire substrate. B: Fused silica substrate.

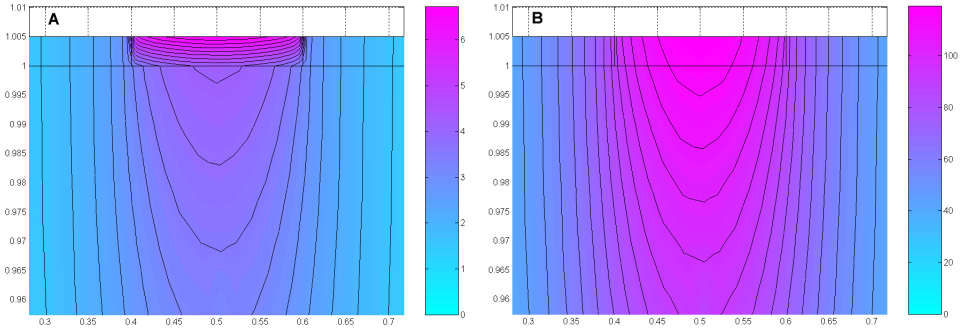

side, so that the isotherms in the coating resemble plane waves until they reach the sapphire. On a fused silica substrate, heat sees the coating and substrate as nearly equivalent materials which diffuse heat at the same rate, so the pattern of isotherms in the coating resemble those in the substrate.

To extrapolate to real mirrors, I choose to model heat flow in the coating separately for these cases. On sapphire ('high-conductivity') substrates, I estimate the coating thermal expansion by treating the heat flow in the coating as purely one-dimensional, and solve for the average temperature of the coating. On fused silica ('low-conductivity') substrates, I use a different method, similar to that introduced in BGV00 [23]. With this technique, I solve for the heat flow in a uniform half-space, and then compute the average temperature for a layer near the surface with a frequency-dependent scale height determined by r_t.

2.4.2.1 High-conductivity substrates

In this model, heat flows much faster in the substrate than in the coating. Therefore heat flow in the coating is essentially one-dimensional, normal to the surface, and because the heat is transmitted directly through the coating, the substrate responds the same as it would without the coating. What then, does one-dimensional heat flow look like? The heat conduction equation is [46]

$$\frac{\partial u(z,t)}{\partial t} - \frac{\kappa}{\rho C_v}\frac{\partial^2 u(z,t)}{\partial z^2} = 0 \tag{2.28}$$

where $u(z)$ is the temperature at depth z and time t. This equation is separable, and has a solution of the form $u(z,t) = u(z)e^{-i\omega t}$. Substitution back into Eq. 2.28 gives

$$i\omega u(z) - \frac{\kappa}{\rho C_v}\frac{\partial^2 u(z)}{\partial z^2} = 0 \tag{2.29}$$

A trial solution of the form $u(z) = u_0 e^{bz}$ determines b.

$$i\omega - \frac{\kappa}{\rho C_v}b^2 = 0 \tag{2.30}$$

$$b = \pm\sqrt{\frac{i\omega\rho C_v}{\kappa}} \tag{2.31}$$

$$u(z,t) \propto e^{i\omega t}\left[c_1 e^{z\sqrt{\frac{i\omega\rho C_v}{\kappa}}} + c_2 e^{-z\sqrt{\frac{i\omega\rho C_v}{\kappa}}}\right] \tag{2.32}$$

where c_1 and c_2 are constants chosen to match the boundary conditions. Since $u(z,t)$ must vanish as $z \to \infty$, we know that $c_1 = 0$. This means that if the surface temperature is given by $u(z = 0, t) = T_0 e^{-i\omega t}$, then the temperature deeper inside the material is

$$u(z = d, t) = T_0 e^{i\omega t} e^{-d\sqrt{\frac{i\omega\rho C_v}{\kappa}}}. \tag{2.33}$$

For photon heating, the boundary conditions specify the derivative of the temperature at the surface. This can be written as [46]

$$\frac{\partial u(z,t)}{\partial t} - \frac{\kappa}{\rho C_v}\frac{\partial^2 u(z,t)}{\partial z^2} = \sum_n \frac{\dot{Q}_n}{\rho C_v}\delta(z - z_n) \tag{2.34}$$

where the amount of heat added is $\dot{Q}$ at location z_n. For the coating on top of a substrate, heat is added by the laser beam at the $z = 0$ surface. Since the substrate has a much greater thermal

diffusivity than the coating, I make the simplifying assumption that the heat flux at the $z = d$ is fully removed from the coating into the substrate. Following [22], and letting $a^2 = \kappa/\rho C_v$, an estimate of the heat flow equation for the coating can be written as

$$\begin{aligned}
(\frac{d}{dt} - a^2\frac{\partial^2}{\partial z^2})u(\vec{r},t) &= \frac{2P(\omega)}{\rho C_v}\left(\delta(z) - \delta(z-d)e^{-d\sqrt{i\omega/a^2}}\right) && (2.35)\\
0 \le z &\le d \\
P(\omega) &= \frac{P_0 e^{i\omega t}e^{-(x^2+y^2)/r_0^2}}{\pi r_0^2} && (2.36)
\end{aligned}$$

In Eq. 2.35, the first δ term accounts for heat added by the laser, and the second δ term accounts for heat flow into the substrate, with a proportionality term from Eq. 2.33. To solve this, we take the Fourier transforms $t \to \omega$ and $z \to k_z$

$$\begin{aligned}
\left(i\omega + a^2k_z^2\right)\tilde{u}(k_z,\omega) &= \frac{2\tilde{P}(\omega)}{\rho C_v}\int_0^\infty \left(\delta(z) - \delta(z-d)e^{-d\sqrt{i\omega/a^2}}\right)e^{ik_z z}\,dz \\
&= \frac{2\tilde{P}(\omega)}{\rho C_v}\left(1 - e^{ik_z d - d\sqrt{i\omega/a^2}}\right) && (2.37)
\end{aligned}$$

Next, invert the spatial transform to solve for the temperature throughout the coating.

$$u(z,\omega) = \frac{2\tilde{P}(\omega)}{\rho C_v}\int_{-\infty}^{\infty}\frac{dk_z}{2\pi}\frac{1 - e^{ik_z d - d\sqrt{i\omega/a^2}}}{i\omega + a^2k^2}e^{-ik_z z} \quad (2.38)$$

Then, average $\bar{u}(\omega)$ over the thickness of the coating by integrating z from 0 to d to calculate the average temperature in the coating.

$$\bar{u}(\omega) = \frac{2\tilde{P}(\omega)}{\rho C_v}\int_0^d\frac{dz}{d}\int_{-\infty}^{\infty}\frac{dk_z}{2\pi}\frac{1 - e^{ik_z d - d\sqrt{i\omega/a^2}}}{i\omega + a^2k^2}e^{-ik_z z} \quad (2.39)$$

Mathematica [125] can evaluate this integral[1], which simplifies to

[1] Use $\int_{-\infty}^{\infty}\frac{1-e^{ik_z d + b\sqrt{id^2\omega/a^2}}}{i\omega + a^2k_z^2}e^{-ik_z z}\,dk$ and let $b \to -1$.

$$\bar{u}(\omega) = \frac{2\tilde{P}(\omega)}{\rho C_v}\frac{1}{d}\frac{\left(1-e^{-d\sqrt{i\omega/a^2}}\right)^2}{i\omega} \tag{2.40}$$

The average displacement the interferometer will see is thus

$$\bar{X}(\omega) = \alpha_{layer} d \int_{-\infty}^{\infty}\int_{-\infty}^{\infty} dx\, dy\, \frac{\bar{u}(\omega)e^{-(x^2+y^2)/r_0^2}}{\pi r_0^2} \tag{2.41}$$

$$= \frac{\alpha_{layer}\tilde{P}(\omega)}{\rho C_v \pi r_0^2 i\omega}\left(1-e^{-d\sqrt{i\omega/a^2}}\right)^2 \tag{2.42}$$

where $\tilde{P}(\omega)$ is the Fourier component of the fluctuations in the light heating the sample. This function approaches zero at low frequencies and Eq. 2.27 at high frequency, within factors of unity. To get the spectral density, we square this and replace $\tilde{P}(\omega)$ with the shot noise spectral density (see §2.4.1).

$$S_{\alpha,P}^{layer}(f) \approx \frac{\alpha_{layer}^2 S_{abs}(f)}{\left(\rho C_v 2\pi^2 r_0^2 f\right)^2}\left(1-e^{-d\sqrt{i2\pi f/a^2}}\right)^4 \tag{2.43}$$

A simple estimate of the layer expansion is

$$\alpha_{layer} = \frac{\alpha_1 d_1}{d_1+d_2} + \frac{\alpha_2 d_2}{d_1+d_2} \tag{2.44}$$

2.4.2.2 Low-conductivity substrates

At high frequencies, where the thermal diffusion length is smaller than the coating thickness, we would expect the coating's photothermal response to act just like a bulk material, only with higher thermal expansion. In the limit of very low frequencies, the whole mirror is essentially isothermal, and the photothermal response should approach a constant value, with the thermal expansion dominated by the substrate. In between, there has to be a transition range, where thermal fluctuations in the coating are transmitted to and diluted by the substrate, but the fluctuations are larger near the surface than they are in the interior of the mirror.

Following BV03, a simple estimate for the temperature of the coating is to assume that the

average heat deposited at the surface is instantly distributed over a volume $V = r_0^2 r_t$ [26, 97]. From the per-cycle change in energy of this volume, $\Delta E \approx P_{abs}/f$, we get the spectrum of its temperature fluctuations.

$$\Delta T_{surface}(f) \approx \frac{\Delta E}{\rho C_v V}$$

Replacing ΔE with P_{abs}/f and V with $\pi r_0^2 r_t$, we get

$$\Delta T_{surface}(f) \approx \frac{P_{abs}(f)}{f \rho C_v r_0^2 r_t}$$

Since $r_t = \sqrt{\kappa/\rho C_v 2\pi f}$, we can write

$$\begin{aligned} \Delta T_{surface}(f) &\approx \frac{P_{abs}(f)}{\pi r_0^2 \sqrt{\rho C_v \kappa 2\pi f}} \\ \bar{X}(f) &= \frac{\alpha_{layer} d P_{abs}(f)}{\pi r_0^2 \sqrt{\rho C_v \kappa 2\pi f}} \end{aligned} \tag{2.45}$$

The spectral density of temperature fluctuations scales with $(\Delta T)^2$, as does the spectral density of the mirror displacement.

$$\begin{aligned} S_{\alpha,P}^{layer*}(f) &= \alpha_{layer}^2 d^2 (\Delta T_{surface}(f))^2 \\ S_{\alpha,P}^{layer*}(f) &= \frac{\alpha_{layer}^2 d^2 S_{abs}(f)}{2\pi^3 r_0^4 \rho C_v \kappa f} \end{aligned} \tag{2.46}$$

where $S_{abs} = P_{abs}^2$. This is intended to demonstrate that, by computing an average temperature near the surface, one finds the spectrum of temperature fluctuations to be proportional to $1/\sqrt{f}$. This clearly does not apply for high frequencies where the coating is not in thermal equilibrium with the substrate, or for low frequencies where the temperature should approach a constant value. A more sophisticated treatment of this problem is derived in the appendix (see §5.1), which arrives at an equation that differs from Eq. 2.46 by a factor of 2.

Eq. 2.46 is proportional to $f^{-1/2}$, while the photothermal response of the substrate scales as

f^{-1}. Comparing this to Eq. 2.27, coating thermal expansion will start to dominate that of the substrate at frequencies above $f_{min} = \frac{\kappa}{\rho C_v d^2} \frac{\alpha_{bulk}^2}{\alpha_{layer}^2}$. Another way of understanding this is that this crossover occurs when $\alpha_{layer} d > \alpha_{bulk} r_t$.

2.4.2.3 Photothermal noise summary

The strength of photothermal noise depends on the thermal properties of the substrate and the coating. The literature (see Table 2.1) suggests that the preferred low-index mirror materials, Al_2O_3 and SiO_2, have low thermal diffusivity, which will dominate the coating's heat conduction. With sapphire and fused silica, the heat flow is expected to be qualitatively different. Fig. 2.1 compares numerical solutions to the heat equation in two dimensions under conditions similar to laser heating. On sapphire, heat flows straight down through the coating under the laser spot. On fused silica, heat diffuses sideways through the coating the same as it does through the substrate.

Shot noise driven photothermal noise is very small, given the low absorption of dielectric mirrors. For the case of LIGO with 800 kW beams, the estimated coating and bulk photothermal noise are plotted in Fig. 2.2.

2.4.3 Coating dn/dT

One would expect length-equivalent photorefractive noise to be like coating thermal expansion noise, substituting αd with $\beta \lambda$. By comparison with Eq. 2.43, we can estimate the photorefractive noise on a fused silica mirror.

$$S_{\beta,P}^{layer}(f) \approx \frac{\beta^2 \lambda^2 S_{abs}(f)}{4\pi^3 r_0^4 \rho C_v \kappa f} \tag{2.47}$$

and for a sapphire mirror,

$$S_{\beta,P}^{layer}(f) \approx \frac{\beta^2 \lambda^2 S_{abs}(f)}{d^2 \left(2\rho C_v \pi^2 r_0^2 f\right)^2} \left(1 - e^{-d\sqrt{i2\pi f/a^2}}\right)^4 \tag{2.48}$$

Figure 2.2: Relative coating and bulk photothermal strain noise in two Advanced LIGO arm cavities. The sapphire line plots coating expansion from Eq. 2.43, and the fused silica line shows the bulk expansion from Eq. 2.26. For coating noise, the end test mirrors (with thicker coatings) dominate. For bulk noise, the input test mirrors (with smaller spot size) dominate. For sapphire, the spot size is taken to be 4.2 cm. For fused silica, the ITM (Input Test Mass) and ETM (End Test Mass) spot sizes (1/e of power) are taken to be 2.5 cm and 3.2 cm [71, 12], respectively. The coating absorption is 0.5 ppm, and the thermal expansion is from the lower values in Table 2.1. The sapphire substrate response is higher than fused silica's because of the difference in thermal expansion coefficients. The predictions of the coating noise use the equations derived in this chapter appropriate to the substrate medium.

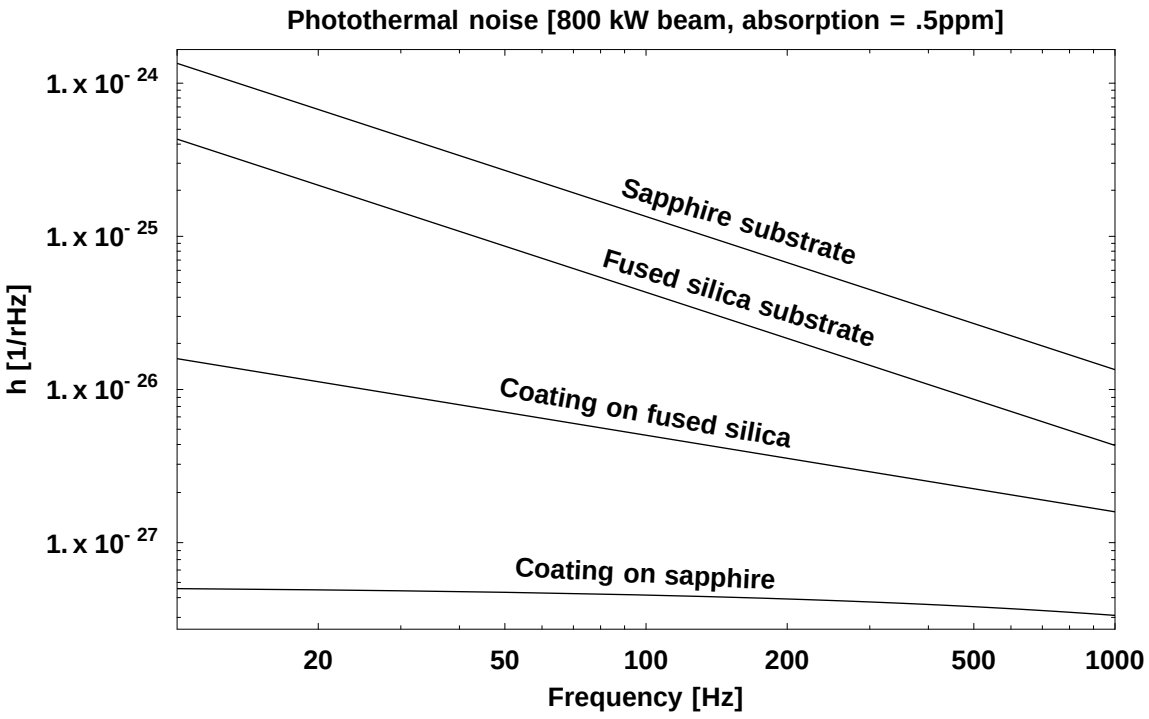

Figure 2.3: Thermal strain noise for LIGO with sapphire and fused silica mirrors. Coating noises are calculated for two ETM mirrors, and bulk noises are calculated for two ITM mirrors. For sapphire mirrors, the spot size is 4.2 cm. For fused silica mirrors, ITM spot size = 2.5 cm, ETM spot size = 3.2 cm. ETM coating = 40 layers, $\alpha_{eff} = 2.4 \times 10^{-6}$.

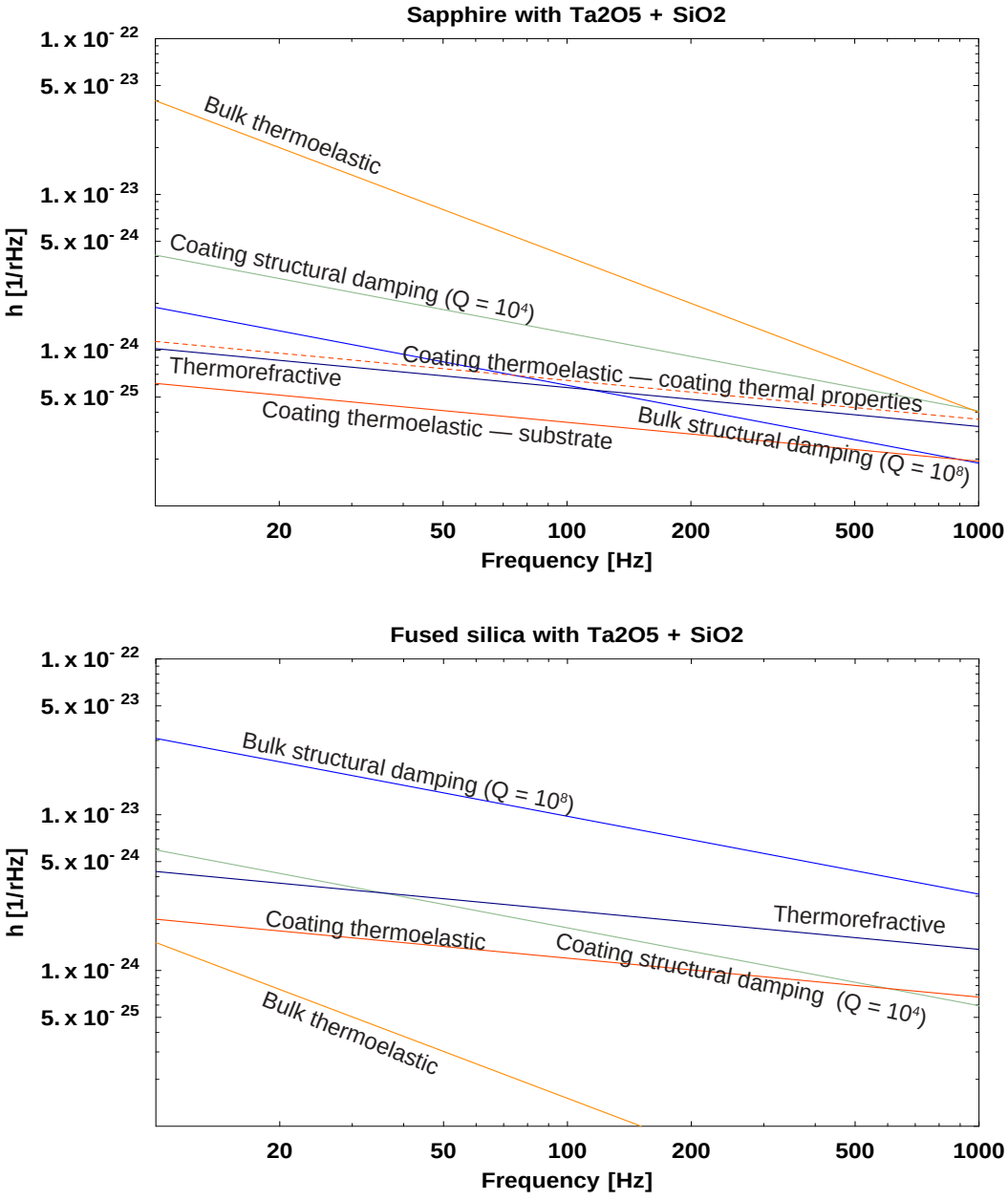

2.5 Summary

Fig. 2.3 shows thermal noise estimates for LIGO. The dominant thermal noise source is predicted to be coating thermoelastic noise given by BV03 (Eq. 2.20), but the theory for this is based on the assumption that the substrate and the coating are thermally coupled. On a sapphire substrate, the coating's low thermal diffusivity may cause it to be essentially decoupled from the substrate. To predict the noise in this case, Eq. 2.20 is plotted using the coating's thermal properties instead of the substrate's. The lower coating thermal expansion coefficients from Table 2.1 are used for this estimate.

Table 2.1: Coating material properties are highly dependent on the manufacturing process. Representative values from the literature are summarized here.

Material	$\alpha \times 10^{-6}$/K	κ W/m-K	E GPa	Sources
TiO_2	50	.25 to 7		[56, 81, 126]
Ta_2O_5	3.6 to -44	.2		[66, 118, 126]
SiO_2	.5 to 4.4	1.1 to 1.7	40 to 77	[68, 89, 81, 122]
Al_2O_3		1.2 to 1.5		[81]

Table 2.2: Summary of noise effects

Source	Symbol	Large-spot length spectral density	Page
Bulk structural damping	$S_{SD}^{bulk}(f)$	$\frac{4k_BT}{(2\pi)^{3/2}f}\frac{\phi(f)(1-\sigma^2)}{E_0 r_0}$	10
Coating structural damping	$S_{SD}^{layer}(f)$	$\frac{2}{\pi^2}\frac{k_BTd}{E_0 r_0^2 f}\left(\frac{E_{coating}}{E_{bulk}}\phi_{\parallel}+\frac{E_{bulk}}{E_{coating}}\phi_{\perp}\right)$	11
Bulk thermoelastic	$S_{\alpha,T}^{bulk}(f)$	$\frac{8}{\sqrt{2\pi}}\frac{\alpha^2(1+\sigma)^2\kappa k_BT^2}{(\rho C_V)^2 r_0^3(2\pi f)^2}$	12
Coating thermoelastic (BV03)	$S_{\alpha,T}^{layer}(f)$	$\frac{4\sqrt{2}}{\pi}\frac{\alpha_{eff}^2(1+\sigma)^2d^2k_BT^2}{r_0^2\sqrt{\kappa\rho C_V 2\pi f}}$	13
Coating thermorefractive	$S_{\beta,T}^{layer}(f)$	$\beta_{eff}^2\lambda^2\frac{\sqrt{2}k_BT^2}{\pi r_0^2\sqrt{2\pi\rho C_v\kappa f}}$	15
Coating photorefractive	$S_{\beta,P}^{layer}(f)$	$\frac{\beta^2\lambda^2 S_{abs}(\omega)}{4\pi^3 r_0^4\rho C_v\kappa f}$	23
Bulk photothermal	$S_{\alpha,P}^{bulk}(f)$	$\frac{\alpha^2(1+\sigma)^2}{2\pi^2}\frac{S_{abs}}{(\rho C_V\pi r_0^2)^2 f^2}$	16
Coating photothermal (sapphire)	$S_{\alpha,P}^{layer}(f)$	$\frac{\alpha_{layer}^2 S_{abs}(f)}{\left(\rho C_v 2\pi^2 r_0^2 f\right)^2}\left(1-e^{-d\sqrt{i2\pi f/a^2}}\right)^4$	18

Table 2.3: Thermal properties of bulk materials. Values given are representative for bulk materials at 300K, and may differ among samples. TiO_2 data are for rutile bulk crystals, C-axis. SiO_2 data are for Corning 7980.

	α	ρ	C_p	κ	σ	r_t	$10\times f_c$
	10^{-6}/K	10^3kg/m^3	J/kg-K	W/m-K		mm @ 100 Hz	Hz @ 1 mm
Al 6061 [40, 6]	23.6	2.7	897	167	.33	.33	110
Ag [85, 6]	18.9	10.5	235	429	.37	.53	280
Au [85, 6]	14.2	19.3	129	317	.42	.45	200
Cu [85, 90]	16.5	8.96	385	401	.36	.43	190
Ti [85, 6]	8.6	4.51	523	21.8	.30	.12	15
GaAs [85, 90]	5.4	5.3	330	56	.31	.23	50
Si [85, 90]	4.68	2.32	702	124	.27	.35	120
Be [85, 6]	11.3	1.85	1825	200	.03	.31	90
TiO_2 [42]	9.19	4.26	711	13	.27	.083	6.8
Al_2O_3 [39]	5	3.98	790	40	.29	.14	20
SiO_2 [35]	.52	2.2	770	1.3	.17	.036	1.5
BK7 [96]	7.1	2.51	858	1.1	.21	.029	.8